The Astrophysical Journal, 584:1120–1126, 2003 February 20

ROLE OF THE HALL CURRENT IN MAGNETOHYDRODYNAMIC DYNAMOS

Pablo D. Mininni and Daniel O. Gómez[1]
Departamento de Física, Facultad de Ciencias Exactas y Naturales, Universidad de Buenos Aires, Ciudad Universitaria, 1428 Buenos Aires, Argentina; mininni@df.uba.ar

and

Swadesh M. Mahajan
Institute for Fusion Studies, University of Texas, Austin, TX 78712
Received 2002 August 2; accepted 2002 October 25

ABSTRACT

A theoretical mean field closure for Hall magnetohydrodynamics (Hall-MHD) is developed to investigate magnetic field generation through dynamo processes in low electron density astrophysical systems. We show that by modifying the dynamics of microscopic flows, the Hall currents could have a profound impact on the generation of macroscopic magnetic fields. As an illustrative example, we show how dynamo waves are modified by the inclusion of Hall currents. By dropping the usual assumption of a correlation time τ for the microscopic dynamics in the mean field dynamos, we find qualitative changes in the growth rate of dynamo modes.
Subject headings: magnetic fields — MHD

1. INTRODUCTION

The standard one-fluid MHD approximation for studying the dynamo activity in astrophysical environments may seriously break down when the kinetic terms contained in the generalized Ohm's law are not negligible. Perhaps the most important of these is the Hall effect (Priest & Forbes 2000) contained in the right-hand side of Ohm's law for an ideal plasma,

$$\boldsymbol{E} + \boldsymbol{u} \times \boldsymbol{B} = \frac{1}{ne}\boldsymbol{j} \times \boldsymbol{B} , \tag{1}$$

where n is the particle density, e is the electron charge, and $\boldsymbol{E}$, $\boldsymbol{u}$, $\boldsymbol{B}$, and $\boldsymbol{j}$ are respectively the electric, velocity, magnetic, and current density vector fields. The Hall current becomes significant when the characteristic length scale L_0 of the system is comparable to the Hall scale

$$L_{\rm H} = \frac{c}{\omega_{\rm pi}}\frac{v_{\rm A}}{V_0} , \tag{2}$$

where c is the speed of light, $v_{\rm A}$ is the Alfvén speed, V_0 is the characteristic speed of the flow, and $\omega_{\rm pi}$ is the ion plasma frequency.

The scales $L_{\rm H}$ and L_0 may become comparable in a number of qualitatively different plasmas. For instance, the Hall scale tends to increase (to approach the macroscopic scale) for low-density fully ionized plasmas or for plasmas with a low degree of ionization ($L_{\rm H}$ scales inversely with charged particle density). It also increases for plasmas in very strong magnetic fields because it is proportional to the Alfvén speed.

Among the astrophysical systems in which Hall effects may be relevant are certain regions of the interstellar medium where the plasma has appropriate characteristic lengths and densities (see, for instance, Spangler 1999). Because $L_{\rm H}$ depends on the mass of the charge carriers, the Hall effect is likely to have a profound influence on the magnetic field dynamics in dense molecular clouds, where relatively massive charged grains form a dynamical plasma component (Wardle & Ng 1999). The Hall effect is also known to strongly affect the Balbus-Hawley magnetorotational instability in weakly ionized accretion disks (Wardle 1999; Balbus & Terquem 2001; Sano & Stone 2002). Norman & Heyvaerts (1985) also noted that the Hall effect may become significant during star formation. Its relevance in compact objects such as white dwarfs and neutron stars is due to the strong magnetic fields observed in these objects (Urpin & Yakovlev 1980; Shalybkov & Urpin 1997; Potekhin 1999). Because of the tiny scales involved, the Hall effect is also relevant in the unsolved problem of the origin and evolution of magnetic fields in the early universe (Tajima et al. 1992).

Notwithstanding this widespread recognition that the Hall effect may be highly relevant, it has not been included in most studies of magnetic field generation by dynamo action. Some exceptions are the studies by Heintzmann (1983) and Galanti, Kleeorin, & Rogachevskii (1994) focused on particular geometries and showing either suppression or enhancement of dynamo action depending on external parameters. In addition, Ji (1999) includes the Hall current in an analysis of the effect of turbulent dynamos on magnetic helicity generation, while Mirnov, Hegna, & Prager (2002) point out the role of the Hall current in enhancing dynamo action in a reversed-field pinch configuration. Finally, de Paor (2001) considers the Hall effect in a simple model of a self-excited dynamo for the Earth's magnetic field.

In a previous paper on the subject (Mininni, Gómez, & Mahajan 2002), it was shown that the Hall-modified α-coefficient could be both qualitatively and quantitatively different from the one predicted by the standard mean field theory (Krause & Rädler 1980); it could be larger or smaller depending on the system. The Hall dynamics tend to modify another standard result of the mean field theory, namely, that the α-effect derived by Pouquet et al. (1976) shuts off when pure Alfvénic states are reached (Gruzinov & Diamond 1994). We find that the new α-effect is generally not quenched by Alfvénic states, suggesting that the

[1] Also at the Instituto de Astronomía y Física del Espacio, Ciudad Universitaria, 1428 Buenos Aires, Argentina.

saturation of a Hall dynamo is likely to be quite different from that of a regular kinematic dynamo. In summary, there seems to be a clear-cut indication that the impact of the Hall effect on dynamo activity in low electron density plasmas must be seriously explored.

In §§ 2 and 3 of the present paper we develop a closure model for the Hall-MHD or two-fluid equations with the explicit purpose of deriving the effect of small-scale flows on the dynamics of large-scale flows and magnetic fields. Our closure scheme goes beyond the usual treatment in standard mean field theory (Krause & Rädler 1980), which associates a well-defined correlation time τ with small-scale motions. It is worth noting that this more general approach remains valid, regardless of whether the Hall effect is important or not. The generalization is shown in § 6, while in § 5 we present the Hall-modified results for the standard approximation. In § 7 we calculate explicit expressions for dynamo action for a particular model of the microscopic flows, namely, the Arnold-Beltrami-Childress (ABC) flows. Dynamo waves have been traditionally used as a first exercise to show the linear characteristics of dynamo theories in astrophysical scenarios. Although most astrophysical dynamos are expected to operate in nonlinear regimes, it is nonetheless instructive to study the impact of the Hall effect in dynamo waves. A particular application of our closure model to study dynamo waves is therefore shown in § 8. Finally, in § 9 we present the main conclusions of the present paper.

2. THE HALL-MHD EQUATIONS

The ideal and incompressible Hall-MHD description of plasmas is described by the normalized set of the modified induction and Euler equations:

$$\frac{\partial \boldsymbol{B}}{\partial t} = \nabla \times [(\boldsymbol{U} - \nabla \times \boldsymbol{B}) \times \boldsymbol{B}] , \quad (3)$$

$$\frac{\partial \boldsymbol{U}}{\partial t} = \boldsymbol{U} \times (\nabla \times \boldsymbol{U}) + (\nabla \times \boldsymbol{B}) \times \boldsymbol{B} - \nabla\left(P + \frac{U^2}{2}\right) , \quad (4)$$

where the velocity and magnetic fields are scaled to a characteristic speed V_0 and lengths are in units of the Hall length $L_{\rm H}$ (i.e., $L_0 = L_{\rm H}$) defined in equation (2). These equations display, among other properties, the freezing of the magnetic field to the electron flow,

$$\boldsymbol{U}^e = \boldsymbol{U} - \nabla \times \boldsymbol{B} , \quad (5)$$

rather than to the bulk velocity field $\boldsymbol{U}$. Since the Hall term, in some sense, is a measure of this difference, these two velocities can be quite different. Consequently, the Hall term is likely to exert a major influence on the generation of the magnetic field through dynamo activity. We are therefore interested in finding out whether this system is able to generate a macroscale magnetic field from an initial microscale configuration, consisting of a small seed magnetic field along with a substantial velocity field.

3. THE CLOSURE MODEL

Our closure, although differently motivated, has features in common with the RSA (reduced smoothing approximation) recently proposed in Blackman & Field (1999; Field, Blackman, & Chou 1999 as well). These closure schemes are much better suited to deal with systems for which the Reynolds number or the Strouhal number is not constrained to be much smaller than unity as compared to the first-order smoothing approximation, the standard closure scheme of the traditional mean field dynamo theories.

Just as in Blackman & Field (1999), we assume the initial state to consist of only small-scale fields $\boldsymbol{u}^0$ and $\boldsymbol{b}^0$, which solve equations (3) and (4). In § 7 we propose and discuss a particular set of solutions, but for now, let us perturb the system about a general microscale state:

$$\boldsymbol{B} = \overline{\boldsymbol{B}} + \boldsymbol{b} + \boldsymbol{b}^0 , \quad (6)$$

$$\boldsymbol{U} = \overline{\boldsymbol{U}} + \boldsymbol{u} + \boldsymbol{u}^0 , \quad (7)$$

where the overbar denotes spatially or statistically averaged large-scale perturbations. Therefore, from equation (5) we can also write the electron flow as

$$\boldsymbol{U}^e = \overline{\boldsymbol{U}}^e + \boldsymbol{u}^e + \boldsymbol{u}^{0,e} , \quad (8)$$

where $\overline{\boldsymbol{U}}^e = \overline{\boldsymbol{U}} - \nabla \times \overline{\boldsymbol{B}}$ is the large-scale electron flow, $\boldsymbol{u}^e = \boldsymbol{u} - \nabla \times \boldsymbol{b}$, and $\boldsymbol{u}^{0,e} = \boldsymbol{u}^0 - \nabla \times \boldsymbol{b}^0$. Note that $\boldsymbol{u} + \boldsymbol{u}^0$, $\boldsymbol{u}^e + \boldsymbol{u}^{0,e}$, and $\boldsymbol{b} + \boldsymbol{b}^0$ are small-scale perturbations. While $\boldsymbol{b}^0$ is the small-scale magnetic field in the absence of $\overline{\boldsymbol{B}}$, $\boldsymbol{b}$ is the perturbation when $\overline{\boldsymbol{B}}$ is present, and therefore it does not need to be isotropic. All small-scale fields have zero averages, while their products in general do not. Substituting the expansions given by equations (6) and (7) into equations (3) and (4), using the equation for $\boldsymbol{b}^0$, and taking averages, we find that the evolution of the large-scale fields is determined by

$$\frac{\partial \overline{\boldsymbol{B}}}{\partial t} = \nabla \times \left[\left(\overline{\boldsymbol{U}} - \nabla \times \overline{\boldsymbol{B}}\right) \times \overline{\boldsymbol{B}}\right] + \left(\frac{\partial \overline{\boldsymbol{B}}}{\partial t}\right)^{\rm turb} , \quad (9)$$

$$\frac{\partial \overline{\boldsymbol{U}}}{\partial t} = \overline{\boldsymbol{U}} \times \left(\nabla \times \overline{\boldsymbol{U}}\right) + \left(\nabla \times \overline{\boldsymbol{B}}\right) \times \overline{\boldsymbol{B}} - \nabla\left(\overline{P} + \frac{\overline{U}^2}{2}\right) + \left(\frac{\partial \overline{\boldsymbol{U}}}{\partial t}\right)^{\rm turb} , \quad (10)$$

where

$$\left(\frac{\partial \overline{\boldsymbol{B}}}{\partial t}\right)^{\rm turb} = \left\langle \nabla \times \left(\boldsymbol{u}^{0,e} \times \boldsymbol{b} + \boldsymbol{u}^e \times \boldsymbol{b}^0\right)\right\rangle , \quad (11)$$

$$\left(\frac{\partial \overline{\boldsymbol{U}}}{\partial t}\right)^{\rm turb} = \left\langle \boldsymbol{u} \times \left(\nabla \times \boldsymbol{u}^0\right) + \boldsymbol{u}^0 \times (\nabla \times \boldsymbol{u}) + (\nabla \times \boldsymbol{b}) \times \boldsymbol{b}^0 + \left(\nabla \times \boldsymbol{b}^0\right) \times \boldsymbol{b} - \nabla\left(\boldsymbol{u}^0 \cdot \boldsymbol{u}\right)\right\rangle . \quad (12)$$

Equations (9) and (10) show that the large-scale fields are driven not only by the Hall-MHD dynamics contained in equations (3) and (4) but also by extra terms reflecting the interaction with small-scale fields. The superscript "turb" is used to describe the appropriate averages of bilinear short-scale quantities formed by the interaction of the perturbation with the initial fields. The last term in the induction equation (eq. [9]) can be interpreted as the curl of the electromotive force $\mathscr{E} = \langle \boldsymbol{u}^{0,e} \times \boldsymbol{b} + \boldsymbol{u}^e \times \boldsymbol{b}^0\rangle$ (see eq. [11]) generated by the microscale fields, while the last term in the Navier-Stokes equation (eq. [10]) can be regarded as the net effective force exerted by the microscale fields on the macroscopic flow (see eq. [12]). The expression given in equation (11) is to be compared and contrasted with the standard prediction in the mean field theory, namely,

$$\mathcal{E} = \langle \boldsymbol{u} \times \boldsymbol{b} \rangle = \alpha \overline{\boldsymbol{B}} - \beta \nabla \times \overline{\boldsymbol{B}} \ . \quad (13)$$

One immediately notes that the flow velocity of the standard result is replaced by the electron velocity. This is related to the fact that in Hall-MHD, the field lines are dragged by the electron flow and not by the hydrodynamic flow. The stretching and folding of magnetic field lines in Hall-MHD is a consequence of their advection by the electron velocity field. Therefore, this approximation is expected to be useful in environments where the freezing of field lines to the bulk fluid breaks down because of weak ionization, such as in protostellar disks (Wardle & Ng 1999). Following the approach of the mean field theories (Krause & Rädler 1980), we now derive quantitative expressions for the scalar quantities α and β in terms of the microscopic fields.

We must inform the reader that the quadratic terms in $\boldsymbol{b}$ and $\boldsymbol{u}$ were dropped in equations (11) and (12), as is usually done in mean field theories. Although this is a widespread practice, these terms may not be negligible if the short-scale perturbations grow to finite amplitudes. We plan to study their role in future numerical work.

Subtracting equation (9) from the general induction equation (3) and remembering that $\boldsymbol{u}^0$ and $\boldsymbol{b}^0$ are solutions of the Hall-MHD equations, we obtain the equation for the small-scale perturbed magnetic field $\boldsymbol{b}$:

$$\frac{\partial \boldsymbol{b}}{\partial t} = (\overline{\boldsymbol{B}} \cdot \nabla) \boldsymbol{u}^{0,e} - (\overline{\boldsymbol{U}} \cdot \nabla) \boldsymbol{b}^0 \ . \quad (14)$$

In a similar manner, we can obtain the perturbed Euler equation:

$$\frac{\partial \boldsymbol{u}}{\partial t} = (\nabla \times \boldsymbol{b}^0) \times \overline{\boldsymbol{B}} - (\overline{\boldsymbol{U}} \cdot \nabla) \boldsymbol{u}^0 - \nabla p \ . \quad (15)$$

Concentrating first on computing an expression for α (see eq. [13]), we drop terms involving spatial derivatives of the mean fields, which would only contribute to the β-coefficient. From the divergence of equation (15) and the assumed incompressibility of the flow, we obtain

$$p = -\boldsymbol{b}^0 \cdot \overline{\boldsymbol{B}} \quad (16)$$

for the small-scale pressure perturbation. Substituting this expression into equation (15) yields

$$\frac{\partial \boldsymbol{u}}{\partial t} = (\overline{\boldsymbol{B}} \cdot \nabla) \boldsymbol{b}^0 - (\overline{\boldsymbol{U}} \cdot \nabla) \boldsymbol{u}^0 \ . \quad (17)$$

Equations (14) and (17) describe the dynamics of the anisotropic part of the small-scale fields $\boldsymbol{u}$ and $\boldsymbol{b}$. For given expressions of their isotropic counterparts $\boldsymbol{u}^0$ and $\boldsymbol{b}^0$, equations (14), (17), (9), and (10) are the set of partial differential equations that describe our mean field Hall-MHD model. These equations can be regarded as a closure model of the Hall-MHD equations, which are more general than the kinematic mean field models in two respects: (1) it is a closure of the full set of equations, since the feedback of the microscale is consistently considered on the evolution of both $\overline{\boldsymbol{B}}$ and $\overline{\boldsymbol{U}}$, and (2) the potential role of the Hall current (especially in the dynamics of the microscale) is properly considered.

4. DOUBLE-BELTRAMI EQUILIBRIA

The isotropic part of the small-scale flows (i.e., $\boldsymbol{u}^0$ and $\boldsymbol{b}^0$ in eqs. [14]–[17]) is now modeled by a class of equilibrium solutions of the Hall-MHD equations derivable from a constrained two-fluid variational principle. The solutions are called double-Beltrami states (Mahajan & Yoshida 1998; Yoshida & Mahajan 2002) and are described by the pair of Beltrami conditions

$$\boldsymbol{u}^0 - \nabla \times \boldsymbol{b}^0 = \frac{\boldsymbol{b}^0}{a} \ ,$$
$$\boldsymbol{b}^0 + \nabla \times \boldsymbol{u}^0 = d\boldsymbol{u}^0 \ , \quad (18)$$

expressing rather basic physical laws: (1) the inertialess electrons follow magnetic lines, and (2) ions follow the field lines modified by their vorticity. The parameters a and d measure the magnetic and generalized helicity and for slowly evolving systems are constants of motion labeling the state (Mahajan et al. 2001; Mininni et al. 2002). These equilibria treat velocity and magnetic fields on an equal footing. In addition, they do not require any exact symmetry (as Grad-Shafranov equilibria do) or negligible $\boldsymbol{U}$ and ∇P, as Taylor states do.

Double-Beltrami conditions (i.e., eq. [19]) are always accompanied by the Bernoulli condition:

$$\nabla \left(p_0 + \frac{u_0^2}{2} \right) = 0 \ , \quad (19)$$

where p_0 is the equilibrium pressure. The general solution of equation (19) can be constructed from a linear combination of two single-Beltrami fields,

$$\nabla \times \boldsymbol{b}^0 = \lambda \boldsymbol{b}^0 \ , \quad (20)$$

with the inverse length scales λ determined by

$$\lambda_{\pm} = -\frac{r}{2} \pm \sqrt{\frac{r^2}{4} - s} \ , \quad (21)$$

where $r = 1/a - d$ and $s = 1 - d/a$. For dynamo applications, we are interested in the situation in which the two scales are widely separated. The long scale is associated with the macroscopic scale of the system , $L_{\rm macro}$, while the shorter scales are associated with the turbulence. In our units (i.e., $L_0 = L_{\rm H}$), the root of equation (21) corresponding to the microscale is $\lambda \approx 1$ (λ^{-1} is the short scale), while the other root satisfies

$$\lambda_{\rm macro} \approx \frac{L_{\rm H}}{L_{\rm macro}} \equiv \epsilon \ll 1 \ . \quad (22)$$

To reflect vanishingly small large-scale velocity and magnetic fields, the initial fields are assumed to be purely small scale, given by

$$\nabla \times \boldsymbol{b}^0 = \lambda \boldsymbol{b}^0 \ , \quad (23)$$

$$\boldsymbol{u}^0 = \left(\lambda + \frac{1}{a} \right) \boldsymbol{b}^0 \ . \quad (24)$$

For the present analysis we are explicitly assuming that the magnetic seed is located at the Hall scale ($\lambda \approx 1$), although other regimes (i.e., $\lambda \neq 1$) can also be explored. The parameter ϵ defined in equation (22) therefore controls the degree of scale separation. Note that this assumption (i.e., the Hall effect being dominant at small scales) is useful in astrophysical environments where the Hall length is expected to be small compared to the largest scales of the system (such as accretion disks). However, this approximation might break down in compact objects, since in these scenarios magnetic fields can be huge, and therefore $L_{\rm H}$ can be comparable even to the size of the object (Shalybkov & Urpin 1997).

In what follows, we use these relationships to express $\boldsymbol{u}^0$ and $\boldsymbol{u}^{0,e}$ in terms of $\boldsymbol{b}^0$.

5. ASSUMPTION OF A CORRELATION TIME

One of the standard assumptions in mean field theory (Krause & Rädler 1980) is the existence of a correlation time τ for turbulent small-scale motions, which is much shorter than the typical timescale for large-scale motions. This assumption (hereafter a τ-closure) allows us to approximate equations (14)–(17) by

$$\boldsymbol{b} \simeq \tau\left[(\overline{\boldsymbol{B}}\cdot\nabla)\boldsymbol{u}^{0,e} - (\overline{\boldsymbol{U}}\cdot\nabla)\boldsymbol{b}^0\right] , \quad (25)$$

$$\boldsymbol{u} \simeq \tau\left[(\overline{\boldsymbol{B}}\cdot\nabla)\boldsymbol{b}^0 - (\overline{\boldsymbol{U}}\cdot\nabla)\boldsymbol{u}^0\right] , \quad (26)$$

which converts equations (11) and (12) to

$$\left(\frac{\partial\overline{\boldsymbol{B}}}{\partial t}\right)^{\rm turb} = \tau\left(1-\frac{\lambda}{a}-\frac{1}{a^2}\right)\left\langle\nabla\times\left[(\overline{\boldsymbol{B}}\cdot\nabla)\boldsymbol{b}^0\times\boldsymbol{b}^0\right]\right\rangle , \quad (27)$$

$$\begin{aligned}\left(\frac{\partial\overline{\boldsymbol{U}}}{\partial t}\right)^{\rm turb} = \Big\langle & (\nabla\times\boldsymbol{b}-\lambda\boldsymbol{b})\times\boldsymbol{b}^0 \\ & - \left(\lambda+\frac{1}{a}\right)(\nabla\times\boldsymbol{u}-\lambda\boldsymbol{u})\times\boldsymbol{b}^0 \\ & - \left(\lambda+\frac{1}{a}\right)\nabla(\boldsymbol{u}\cdot\boldsymbol{b}^0)\Big\rangle , \end{aligned} \quad (28)$$

where equations (23) and (24) have been used. Note that the right-hand sides in equations (27) and (28) are linear in the large-scale fields $\overline{\boldsymbol{B}}$ and $\overline{\boldsymbol{U}}$ with the corresponding coefficients as statistical averages of quadratic quantities in the microscale states. More specifically (using the Einstein summation convention),

$$\left(\frac{\partial\overline{\boldsymbol{B}}}{\partial t}\right)^{\rm turb}_i = \tau\left(1-\frac{\lambda}{a}-\frac{1}{a^2}\right)\left(C_{in}\overline{B}_n + A_{ijn}\partial_j\overline{B}_n\right) , \quad (29)$$

$$\begin{aligned}\left(\frac{\partial\overline{\boldsymbol{U}}}{\partial t}\right)^{\rm turb}_i = \tau\Bigg(& -\left(\lambda+\frac{1}{a}\right)D_{in}\left[\overline{B}_n-\left(\lambda+\frac{1}{a}\right)\overline{U}_n\right] \\ & - E_n\partial_i\left(\frac{1}{a}\overline{B}_n-\overline{U}_n\right) \\ & + F_{ikn}\partial_k\left\{\lambda\overline{B}_n+\left[\left(\lambda+\frac{1}{a}\right)^2-1\right]\overline{U}_n\right\}\Bigg) , \end{aligned} \quad (30)$$

where the corresponding coefficients are

$$\begin{aligned} A_{ijn} &= \langle b_j^0\partial_n b_i^0 - b_i^0\partial_n b_j^0\rangle , \\ C_{in} &= \langle b_j^0\partial_{jn}^2 b_i^0 - \partial_n b_j^0\partial_j b_i^0\rangle , \\ D_{in} &= \left\langle\partial_{in}^2\left(\frac{b_0^2}{2}\right)\right\rangle, \quad E_n = \left\langle\partial_n^2\left(\frac{b_0^2}{2}\right)\right\rangle , \\ F_{ikn} &= \langle b_k^0\partial_n b_i^0\rangle . \end{aligned} \quad (31)$$

Once the set of stationary equilibria $\boldsymbol{b}^0(\boldsymbol{x})$ are chosen, the coefficients in equations (31) can be computed, and equations (29) and (30) then close equations (9) and (10).

6. GENERAL APPROACH

The assumption of the existence of a finite correlation time allowed us to replace time derivatives inside averages in § 5. However, this hypothesis (although commonly made in mean field theory) has no theoretical, experimental, or numerical justification. In this section we present an alternative approach to this problem. The expressions on the right-hand side of equations (11) and (12) are linear in both the isotropic ($\boldsymbol{b}^0$, $\boldsymbol{u}^0$) and anisotropic ($\boldsymbol{b}$, $\boldsymbol{u}$) parts of the small-scale fields. Since we are assuming the isotropic part of the fields to correspond to double-Beltrami stationary flows, an extra derivative on equations (11) and (12) simply yields expressions that are now linear in $\boldsymbol{b}^0$, $\boldsymbol{u}^0$, $\partial\boldsymbol{b}/\partial t$, and $\partial\boldsymbol{u}/\partial t$. The general expressions for $\partial\boldsymbol{b}/\partial t$ and $\partial\boldsymbol{u}/\partial t$ are already given by equations (14) and (17). A more general closure, not requiring a correlation time τ, then follows. The new closure conditions are

$$\left(\frac{\partial^2\overline{\boldsymbol{B}}}{\partial t^2}\right)^{\rm turb}_i = \left(1-\frac{\lambda}{a}-\frac{1}{a^2}\right)\left(C_{in}\overline{B}_n + A_{ijn}\partial_j\overline{B}_n\right) , \quad (32)$$

$$\begin{aligned}\left(\frac{\partial^2\overline{\boldsymbol{U}}}{\partial t^2}\right)^{\rm turb}_i = \Bigg(& -\left(\lambda+\frac{1}{a}\right)D_{in}\left[\overline{B}_n-\left(\lambda+\frac{1}{a}\right)\overline{U}_n\right] \\ & - E_n\partial_i\left(\frac{1}{a}\overline{B}_n-\overline{U}_n\right) \\ & + F_{ikn}\partial_k\left\{\lambda\overline{B}_n+\left[\left(\lambda+\frac{1}{a}\right)^2-1\right]\overline{U}_n\right\}\Bigg) , \end{aligned} \quad (33)$$

where all coefficients are given by equations (31). The price paid for this generality is the appearance of higher order derivatives (second-order derivatives on the left-hand sides of eqs. [32] and [33]) in the closure conditions. Note also that these expressions rely on the assumption of double-Beltrami equilibria, which determine the morphology of the magnetic seed. Below we explore the limits of validity of the "correlation time" assumption in the propagation of dynamo waves.

7. MICROSCOPIC STATES: ABC FLOWS

Let us complete the calculation using an explicit representation of the double-Beltrami flows; the small-scale fields are taken to be isotropic ABC flows, which are helical Beltrami states given by

$$\begin{aligned}\boldsymbol{b}^0 = b_0\{ & [\cos(\lambda y)+\sin(\lambda z)]\hat{\boldsymbol{x}} + [\cos(\lambda z)+\sin(\lambda x)]\hat{\boldsymbol{y}} \\ & + [\cos(\lambda x)+\sin(\lambda y)]\hat{\boldsymbol{z}}\} . \end{aligned} \quad (34)$$

By straightforward computations, we find the coefficients listed in equations (31) to be

$$\begin{aligned} A_{ikn} &= 2F_{ikn}, \quad C_{in} = 0 , \\ D_{in} &= 0, \quad E_n = 0 , \\ F_{ikn} &= \frac{b_0^2}{2}\left(\delta_{k+1,i-1}\delta_{n,i-1} - \delta_{k-1,i+1}\delta_{n,i+1}\right) , \end{aligned} \quad (35)$$

converting our closure conditions to the coupled set

$$\left(\frac{\partial^2 \overline{\boldsymbol{B}}}{\partial t^2}\right)^{\rm turb} = b_0^2\left(1 - \frac{\lambda}{a} - \frac{1}{a^2}\right)\nabla \times \overline{\boldsymbol{B}} \,, \qquad (36)$$

$$\left(\frac{\partial^2 \overline{\boldsymbol{U}}}{\partial t^2}\right)^{\rm turb} = \frac{b_0^2}{2}\left[\left(\lambda + \frac{1}{a}\right)^2 - 1\right]\nabla \times \overline{\boldsymbol{U}} - \frac{b_0^2}{2}\lambda\nabla \times \overline{\boldsymbol{B}} \,. \qquad (37)$$

Closure equations (36) and (37) express the evolution of large-scale flows and magnetic fields driven by microscale dynamics. In particular, equation (36) is a generalized version of the α-effect, since we are not assuming any correlation time. The standard α-effect can be recovered by assuming a correlation time τ, reducing equation (36) to

$$\left(\frac{\partial \overline{\boldsymbol{B}}}{\partial t}\right)^{\rm turb} = \alpha\nabla \times \overline{\boldsymbol{B}} \,, \qquad (38)$$

where

$$\alpha = \tau\alpha_0 = \tau b_0^2\left(1 - \frac{\lambda}{a} - \frac{1}{a^2}\right) . \qquad (39)$$

The properties of this expression of the coefficient α and its comparison with results arising from other mean field models have been explored elsewhere (Mininni et al. 2002). Note that these closure conditions (i.e., eqs. [36] and [37]) go beyond the framework of a kinematic dynamo model and correspond to a full Hall-MHD dynamo.

We can also compute the coefficient β defined in equation (13) by following the procedure used for evaluating α. Retaining first-order spatial derivatives of $\overline{\boldsymbol{B}}$ in equations (14) and (15), we obtain

$$\beta = \tau\beta_0 = \frac{\tau b_0^2}{3}\left[1 + \left(\lambda + \frac{1}{a}\right)^2\right] . \qquad (40)$$

The role of β in equation (9) is to provide an enhanced magnetic diffusivity. It has, for instance, an important impact on the dispersion relationship of dynamo waves, as shown in § 8.

8. HALL EFFECT ON DYNAMO WAVES

Just as an illustrative example of how the Hall term might affect dynamo activity, let us apply our closure model (eqs. [9], [10], [32], and [33]) to determine the dispersion relationship of dynamo waves. Although the linear approximation used in this section is expected to break down in astrophysical dynamos, studying the properties of dynamo waves is still useful for assessing the role of the Hall effect in the generation of magnetic fields. To this end, we consider a slab geometry for the macroscopic field (following Zweibel 1988), i.e.,

$$\overline{\boldsymbol{U}} = \hat{\boldsymbol{x}}\Omega y \,, \qquad (41)$$

representing the Ω-effect in Cartesian geometry. In our dimensionless version, $\Omega = 1$. We perturb this shear flow with a large-scale magnetic field:

$$\overline{\boldsymbol{B}} = \hat{\boldsymbol{x}}B_x(z,\ t) + \hat{\boldsymbol{y}}B_y(z,\ t) \,. \qquad (42)$$

Assuming

$$\overline{\boldsymbol{B}}(z,\ t) \approx \exp(pt + ikz) \,, \qquad (43)$$

the linearized equation (9) yields

$$\begin{pmatrix} p + \beta_0 k^2 & \dfrac{ik\alpha_0}{p} - 1 \\ \dfrac{ik\alpha_0}{p} & p + \beta_0 k^2 \end{pmatrix}\begin{pmatrix} B_x \\ B_y \end{pmatrix} = 0 \,, \qquad (44)$$

where α_0 is defined in equation (39). The corresponding dispersion relationship is

$$\left(p + \beta_0 k^2\right)^2 = \left(\frac{k\alpha_0}{p}\right)^2 + \frac{ik\alpha_0}{p} \,, \qquad (45)$$

which is a fourth-order polynomial in p. Out of the four roots of equation (45), only one of them has $\mathrm{Re}(p) > 0$, which therefore corresponds to spontaneously growing dynamo waves. Both the growth rate and frequency of this unstable branch are plotted in Figure 1 as a function of the wavenumber.

In Figure 1 (*top*) we show the growth rate [i.e., $\mathrm{Re}(p)$] as a function of wavenumber. The coefficients α_0 and β_0 in

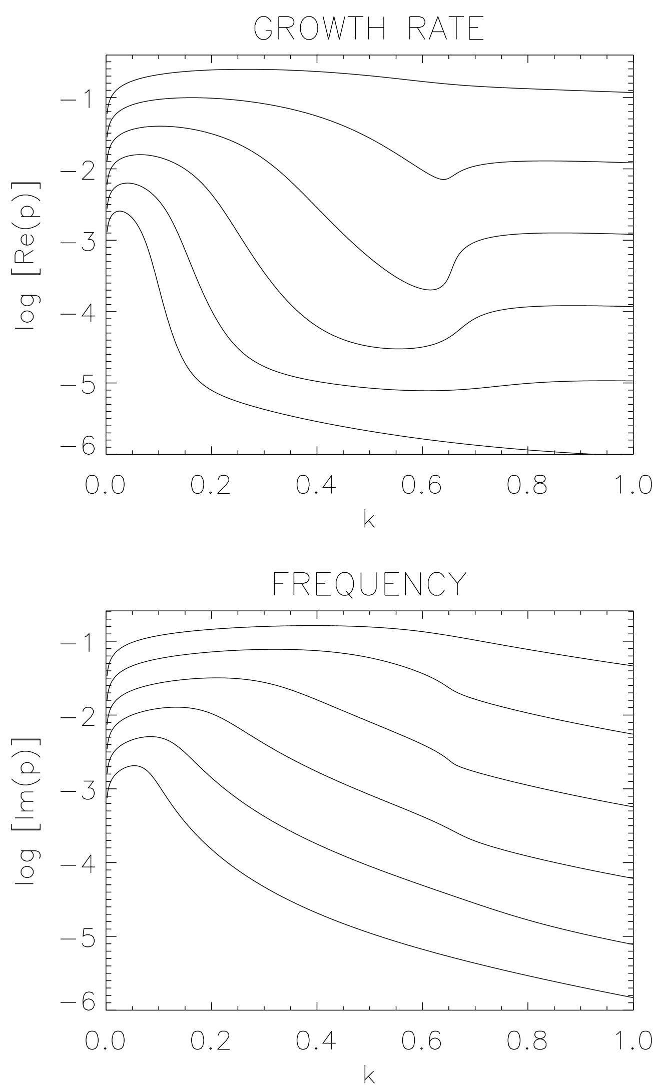

FIG. 1.—(*a*) Growth rate vs. wavenumber for dynamo waves for $\epsilon = 10^{-1}, 10^{-2}, \ldots, 10^{-6}$, starting from the top. (*b*) Same as (*a*), but for the frequency of dynamo waves. In all these cases $b_0^2 = 1$.

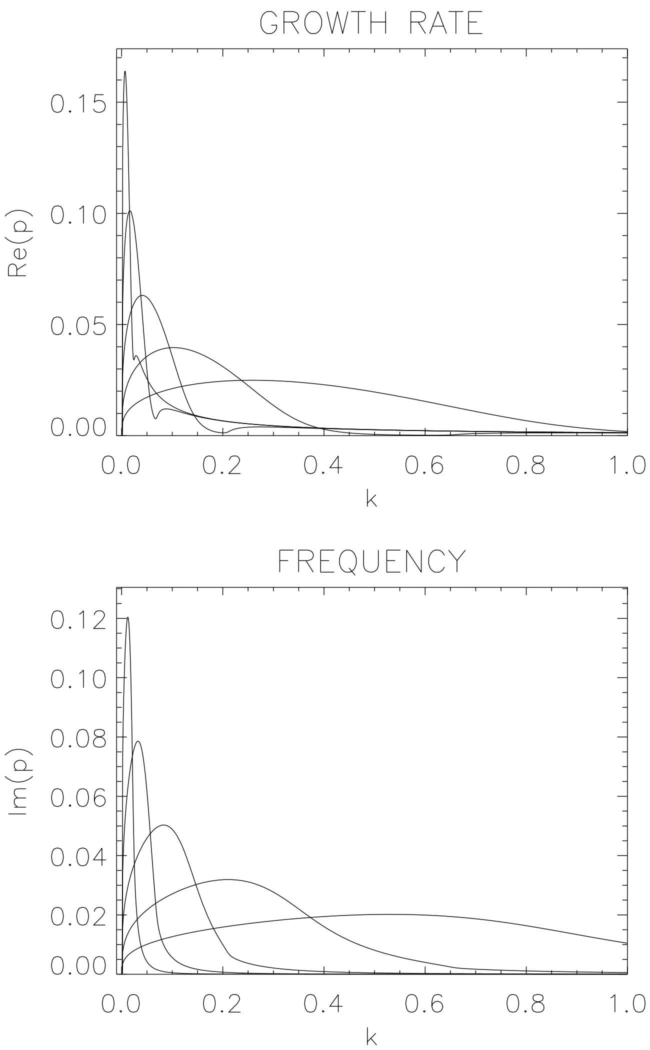

FIG. 2.—(*a*) Growth rate vs. wavenumber for $b_0^2 = 10^3$, 10^2, 10^1, 10^0, and 10^{-1}, starting from the top. (*b*) Same as (*a*), but for the corresponding frequency. In all these cases $\epsilon = 10^{-3}$.

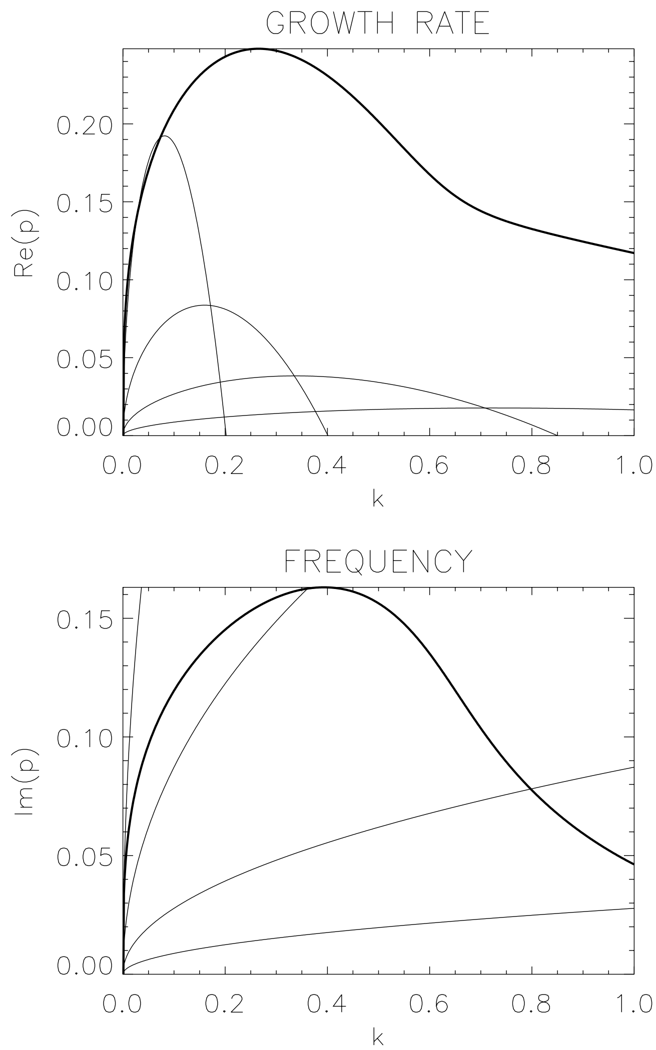

FIG. 3.—(*a*) Growth rate vs. wavenumber for $\epsilon = 0.1$ and $b_0^2 = 1$. The thick line corresponds to the general closure given by eq. (45). Thin lines correspond to a τ-closure given by eq. (46) and $\tau = 10^1$, 10^0, 10^{-1}, and 10^{-2}, starting from the top. (*b*) Same as (*a*), but for the corresponding frequency.

equation (45) depend on two free parameters: (1) the scale separation given by ϵ (see eq. [22]) and (2) the intensity of the microscopic ABC equilibrium measured by b_0^2 (see eq. [34]). This figure shows that this dynamo mode is unstable at all wavenumbers. Note that in this approximation, the Hall scale coincides with the microscale, $L_{\rm H} \approx L_0$. As the scale separation increases (i.e., $\epsilon \to 0$), $L_{\rm macro} \gg L_0 \approx L_{\rm H}$, and therefore the growth rate is reduced. Both the maximum growth rate and the wavenumber at which this maximum is attained scale as $\sqrt{\epsilon}$. Figure 1 (*bottom*) shows the time frequency [i.e., Im(p)] for this mode as a function of wavenumber.

Figure 2 shows the effect of changing the equilibrium intensity b_0^2 on both the growth rate (Fig. 2 [*top*]) and the frequency (Fig. 2 [*bottom*]). While the most unstable wavenumber scales as $1/b_0^{1/2}$, the maximum growth rate scales as $b_0^{1/2}$.

If a characteristic correlation time τ is assumed for the microscale, we recover the well-known mean field dispersion relation,

$$\left(p_\tau + \tau\beta_0 k^2\right)^2 = (k\tau\alpha_0)^2 + ik\tau\alpha_0 \ , \qquad (46)$$

a quadratic polynomial in p_τ, but again with only one unstable branch. This relationship contains two asymptotic regimes dictated by the term that dominates the right-hand side: (1) the α^2 regime, for $k\alpha \gg \Omega$ (in our notation it is $\alpha = \tau\alpha_0$ and $\beta = \tau\beta_0$), and (2) the α-Ω regime, for $k\alpha \ll \Omega$.

In Figure 3 we compare the dispersion relation arising from equation (45) and the one arising from a τ-closure (see eq. [46]). According to the τ-closure, the region of unstable modes ranges from $k = 0$ to $k_{\rm max}$ ($k_{\rm max}$ scales with τ as $k_{\rm max} \approx \tau^{-1/3}$). This is different from the prediction of the more general closure, according to which all wavenumbers remain unstable. Furthermore, regardless of the value chosen for τ, both the growth rate and frequency curves behave fundamentally differently from the prediction given by the general closure.

9. CONCLUSIONS

In this paper we have conducted a preliminary examination of the effects of Hall currents on dynamo activity, which are neglected in MHD models. We have developed a closure scheme (resembling RSA in MHD) pertinent to a variety of astrophysical plasmas for which the Reynolds number and/or the Strouhal number could be arbitrarily large. It is important to emphasize that our general closure deviates from the standard practice of invoking the existence of a particular correlation time τ for the microscale dynamics. This leads to higher order dynamical equations for the evolution of the macroscopic fields. A principal contribution of the Hall currents is the creation of microscale fields that can have a strong impact on the dynamics of the macroscopic fields and flows (see eqs. [9] and [10]).

The main results of the present paper are the general expressions of our closure model, given in equations (36) and (37). To obtain specific predictions from this closure for particular astrophysical problems, we need to integrate the Hall-MHD macroscopic equations (i.e., eqs. [9] and [10]) with the appropriate physical and geometrical assumptions. This task is beyond the scope of the present analysis. However, to illustrate the potential capabilities of this closure model, we calculated the dispersion relation of dynamo waves in Cartesian geometry. The linearized equations were solved to investigate the nature of dynamo waves in the presence of Hall currents. We found that the spectrum as well as the growth rates of the dynamo waves are considerably different from their MHD counterparts. We also showed how the dynamo waves in the general closure model differ from what they could be in a τ-closure model. For instance, according to the general closure all wavenumbers remain unstable, while for a τ-closure the region of unstable modes ranges from $k = 0$ to $k_{\max}$, where $k_{\max}$ scales inversely with τ.

As mentioned in § 1, although there is an extensive list of astrophysical systems in which the Hall effect is potentially relevant, theoretical studies about the origin of magnetic fields in these plasmas usually neglect this effect. We therefore believe that a sustained effort is required to overcome this theoretical deficiency. The present paper is one step in this direction, which adds to previous studies on Hall dynamos (Heintzmann 1983; Galanti et al. 1994; Mirnov et al. 2002; de Paor 2001; Sano & Stone 2002; Ji 1999; Mininni et al. 2002).

The preliminary results presented in this paper strongly suggest that the impact of Hall currents on dynamo action in low electron density astrophysical plasmas must be carefully explored. The detailed study of this and other relevant issues, such as the nonlinear saturation of dynamo action, is the subject matter of a forthcoming paper based on numerical simulations of Hall-mediated dynamos (Mininni, Gómez, & Mahajan 2003).

The authors are very grateful to the Abdus Salam International Centre for Theoretical Physics, where the initial stages of this study were performed. P. D. M. is a fellow of CONICET, and D. O. G. is a member of the Carrera del Investigador del CONICET. P. D. M. and D. O. G. acknowledge support from the University of Buenos Aires through grant X209/00, and S. M. M. from US Department of Energy contract DE-FG03-96ER-54366.

REFERENCES

Balbus, S. A., & Terquem, C. 2001, ApJ, 552, 235
Blackman, E. G., & Field, G. B. 1999, ApJ, 521, 597
de Paor, A. 2001, Nonlinear Proc. Geophys., 8, 265
Field, G. B., Blackman, E. G., & Chou, H. 1999, ApJ, 513, 638
Galanti, B., Kleeorin, N., & Rogachevskii, I. 1994, Phys. Plasmas, 1, 3843
Gruzinov, A., & Diamond, P. H. 1994, Phys. Rev. Lett., 72, 1651
Heintzmann, H. 1983, J. Exp. Theor. Phys., 57, 251
Ji, H. 1999, Phys. Rev. Lett., 83, 3198
Krause, F., & Rädler, K.-H. 1980, Mean Field Magnetohydrodynamics and Dynamo Theory (New York: Pergamon)
Mahajan, S. M., Miklazewski, R., Nikolskaya, K., & Shatashvili, N. 2001, Phys. Plasmas, 8, 1340
Mahajan, S. M., & Yoshida, Z. 1998, Phys. Rev. Lett., 81, 4863
Mininni, P. D., Gómez, D. O., & Mahajan, S. M. 2002, ApJ, 567, L81
———. 2003, ApJ, submitted
Mirnov, V. V., Hegna, C. C., & Prager, S. C. 2002, Presentation at Intl. Sherwood Fusion Theory Conf.
Norman, C., & Heyvaerts, J. 1985, A&A, 147, 247
Potekhin, A. Y. 1999, A&A, 351, 787
Pouquet, A., Frisch, U., & Leorat, J. 1976, J. Fluid Mech., 77, 321
Priest, E. R., & Forbes, T. 2000, Magnetic Reconnection: MHD Theory and Applications (New York: Cambridge Univ. Press)
Sano, T., & Stone, J. M. 2002, ApJ, 570, 314
Shalybkov, D. A., & Urpin, V. A. 1997, A&A, 321, 685
Spangler, S. R. 1999, in Proc. 2nd Guillermo Haro Conf., Interstellar Turbulence, ed. J. Franco & A. Carraminana (Cambridge: Cambridge Univ. Press), 41
Tajima, T., Cable, S., Shibata, K., & Kulsrud, R. M. 1992, ApJ, 390, 309
Urpin, V. A., & Yakovlev, D. 1980, AZh, 24, 303
Wardle, M. 1999, MNRAS, 307, 849
Wardle, M., & Ng, C. 1999, MNRAS, 303, 239
Yoshida, Z., & Mahajan, S. M. 2002, Phys. Rev. Lett., 88, 095001
Zweibel, E. G. 1988, ApJ, 329, 384